Intensity asymmetry in the Mossbauer spectra of a layered cyanide

1990 J. Phys.: Condens. Matter 2 7209

(http://iopscience.iop.org/0953-8984/2/34/014)

J. Phys.: Condens. Matter **2** (1990) 7209–7223. Printed in the UK

Intensity asymmetry in the Mössbauer spectra of a layered cyanide

S Das, S Ganguli and M Bhattacharya
Saha Institute of Nuclear Physics, 92 Acharya Prafulla Chandra Road, Calcutta 700 009, India

Received 15 August 1989, in final form 1 January 1990

Abstract. Results of ^{57}Fe Mossbauer investigation in a layered cyanide $Mg[Mg((CH_2)_6N_4)_2Fe(CN)_6]_2 . nH_2O$ for different stages of hydration are presented. Mössbauer spectra in the partially hydrated stages show an asymmetry in the intensity of the two absorption peaks of the quadrupolar doublet. The powder pattern has been analysed in terms of superposition of two asymmetric doublets arising from two inequivalent sites. An explanation for the asymmetry of the intensity in the doublet spectrum has been suggested in terms of the Goldanskii–Karyagin effect.

1. Introduction

Layered materials (Wilson and Yoffe 1969, Wilson *et al* 1975, Schollhorn 1980) are characterised by strong bonding between atoms within the layer while a weak van der Waals force acts perpendicular to it. Graphite transition-metal dichalcogenides, silicates and metal cyanides belong to this class. Layered transition-metal dichalcogenides, a typical example of layered material of the form MX_2, consist of a three-sheet system, where the metal sheet M (M ≡ transition metals) is sandwiched between two chalcogen sheets X (X ≡ S, Se, Te) and the two dimensionally infinite MX_2 layers are held together in the bulk solid by a weak van der Waals force. The metal atoms occupy lattice sites of octahedral or trigonal prismatic symmetry. Various guest species such as alkali metals, transition metals and a large number of inorganic and organic molecules may enter (intercalate) into the van der Waals gap and cause lattice expansion and other drastic changes in the physical properties of the material as a result of charge transfer between the host layer and the guest (Whittingham 1978, Whittingham and Jacobson 1982, Levy 1979). Compared with other materials, layered cyanides remained neglected for a long time. The layered cyanide (Weiss *et al* 1953), magnesium hexamethylene tetramine hexacyanoferrate(III) has the chemical formula $Mg(X)_n . [Mg((CH_2)_6N_4)_2 . Fe(CN)_6]_2$ (X ≡ water). In the previous communication (Das *et al* 1985) the structural aspects of this cyanide have been compared with layered transition-metal dichalcogenides (figure 1). All the water molecules and one third of the Mg^{2+} ions reside in the van der Waals space. With gradual heating, the water molecules are expelled from the compound in steps, giving rise to a structural change from the tetragonal in the hydrated form to cubic in the dehydrated form. In fact, the compound is capable of attaining the hydrated form with 24, 22, 17, 12, nine or seven water molecules. In our earlier communication the

0953-8984/90/347209 + 15 $03.50

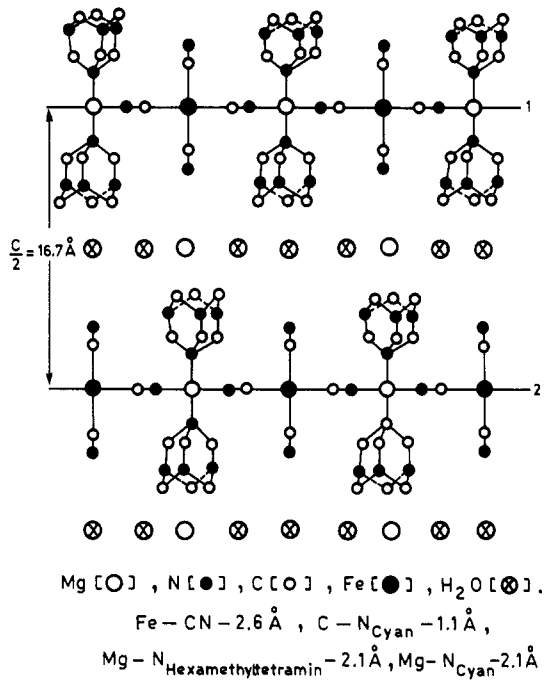

Figure 1. Schematic crystal structure of $Mg[Mg((CH_2)_6N_4)_2Fe(CN)_6].nH_2O$.

single-line and the doublet spectra obtained in the limiting cases (completely hydrated and completely dehydrated states) have been attributed to low-spin Fe(II) and low-spin Fe(III), respectively, invoking the nucleophilic effect of water molecules on $Fe(CN)_6$ in the specimen where only the equivalent site for Fe has been assumed, but the results of the present investigation in the intermediate stages uphold the existence of two inequivalent sites characterised by different isomer shifts. Moreover, the isomer shifts for the two sites as a function of water content of the material change in opposite directions. This comes into conflict with the earlier interpretation where the nucleophilic effect has been emphasised. The present work attempts to put forward an alternative explanation without introducing a dramatic change in the oxidation state of iron. Moreover, the spectra of the samples treated at intermediate temperatures show an asymmetry in the intensity of the two absorption peaks of the quadrupole doublet. The present paper also strives to offer an explanation for the asymmetry of the intensity of the spectra and estimates Mössbauer parameters on the basis of structural details.

2. Experimental details

The ^{57}Fe Mössbauer spectra were recorded in horizontal transmission geometry, using a constant-acceleration spectrometer (Wissel 1000) coupled with a model 7100 multichannel analyser (E G & G Ortec). A 10 mCi ^{57}Co source in a Rh matrix from Amersham was used. The velocity was calibrated using a metallic iron absorber. Data were collected at low temperatures with a liquid-nitrogen cryostat using the continuous-flow technique

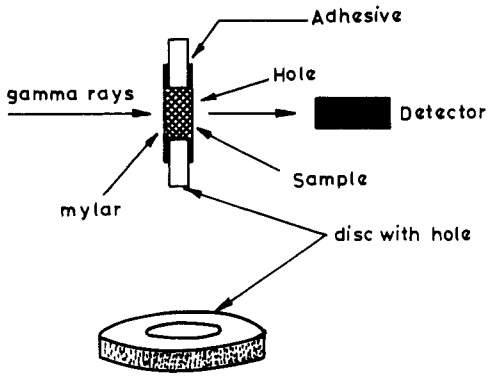

Figure 2. Diagram of the experimental arrangements and the sample holder.

(Das *et al* 1983). Figure 2 shows the diagram of the experimental arrangement and the sample holder. The sample which was placed in the holder and held between two Mylar films was heated at a fixed temperature for $\frac{1}{2}$ h. The water molecules were expelled through a hole in the Mylar film and finally the hole was sealed with a small amount of adhesive. The Mössbauer spectra of these samples at different stages of hydration were recorded at ambient temperature.

The DC conduction of the sample in the form of pressed pellet (12 mm diameter and about 1.5 mm thickness) was measured with the pellet held rigidly between two electrodes by a screw arrangement. The electrodes were connected to an electrometer (Keithley Instruments model 610c). The temperature of the sample was increased at the rate of 2 °C min^{-1}. The method of the sample preparation has been described elsewhere (Weiss *et al* 1953, Das *et al* 1985).

3. Results and discussion

3.1. Resistivity

In figure 3 we have plotted the logarithm of the resistance against inverse temperature. The curve follows two straight lines with different slopes, i.e. in each part the resistivity ρ follows an exponential law. In the high-temperature range the activation energy is 0.36 eV and in the low-temperature range the activation energy is 0.15 eV.

3.2. Mössbauer spectral features

The Mössbauer spectra of two extreme cases (the completely hydrated and completely dehydrated cases) have been presented earlier (Das *et al* 1985). The Mössbauer spectrum of the completely hydrated compound exhibits a single line and that of the completely dehydrated compound shows a doublet with a quadrupole splitting corresponding to the Fe(III) ion in ferricyanides. Figure 4 presents the Mössbauer spectra of the compound in the intermediate stages of hydration between the fully hydrated and fully dehydrated stages. It is observed from the figure that a quadrupole splitting develops in the spectra with gradual dehydration and this splitting finally reaches a value which is typical of low-spin ferricyanide when the sample is treated at about 100 °C under vacuum. Figure 5 presents the spectra of the rehydrated samples which were prepared from the dehydrated

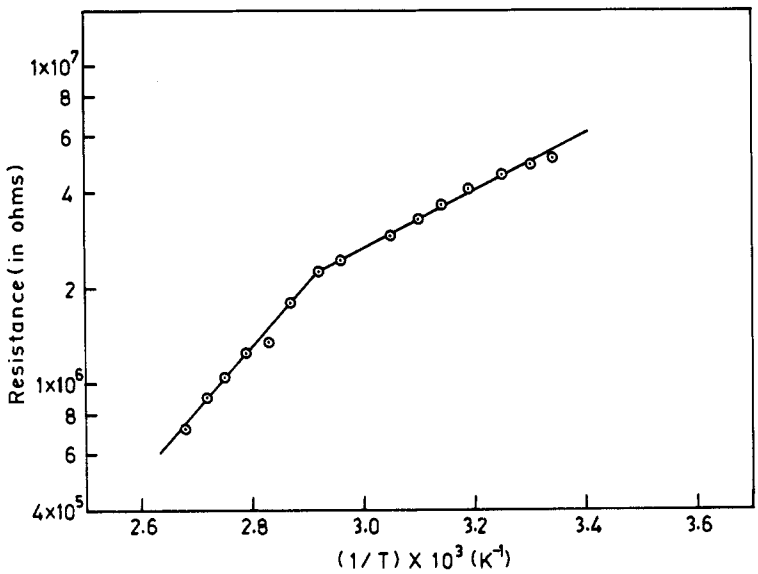

Figure 3. Resistance of $Mg[Mg((CH_2)_6N_4)_2Fe(CN)_6]_2 . nH_2O$ as a function of inverse temperature.

specimen by keeping it under water for different durations of time and shows how the quadrupole-split doublet gradually collapses into a single line on increase in the number of intercalated water molecules. These two figures uphold the reversibility of the inclusion and exclusion of water molecules. Therefore, figures 4 and 5 exhibit continuous development of splitting with dehydration and gradual collapse of the splitting with rehydration, respectively. Although marked differences are observed in the spectral shape for the intermediate stages in the two cases, the spectra in the two limiting cases in both the figures are almost identical.

Detailed inspection reveals that the spectra for the limiting cases as presented in figures 4 and 5 contain differences arising from slight inequality of the state of hydration of the samples. It should be mentioned here that figure 4, spectrum E, and figure 5, spectrum A, represent samples which have different treatment conditions. The sample for figure 4, spectrum E, was treated at 100 °C and it had seven molecules of water still present in it whereas the sample for figure 5, spectrum A, was treated at 100 °C under vacuum and was almost completely dehydrated. As a result figure 5, spectrum A, shows a larger quadrupole splitting than that presented in figure 4, spectrum E (Das *et al* 1985). Spectrum E in figure 5 is wider than that of the completely hydrated sample, indicating that the hydration is not yet complete.

It is to be noted that the spectra for the intermediate stages during dehydration and rehydration as shown in figures 4 and 5 are quite dissimilar. This can be explained in the following way. The thermogravimetric analysis (TGA) shows that the water molecules come out of the sample in steps, indicating that there exist different groups of water molecules characterised by different bonding energies and by different locations in the fully hydrated specimen. The treatment temperatures were chosen somewhere in the middle of the temperature span of each step. In order to achieve different degrees of dehydration the sample was kept at various temperatures for a certain duration. During

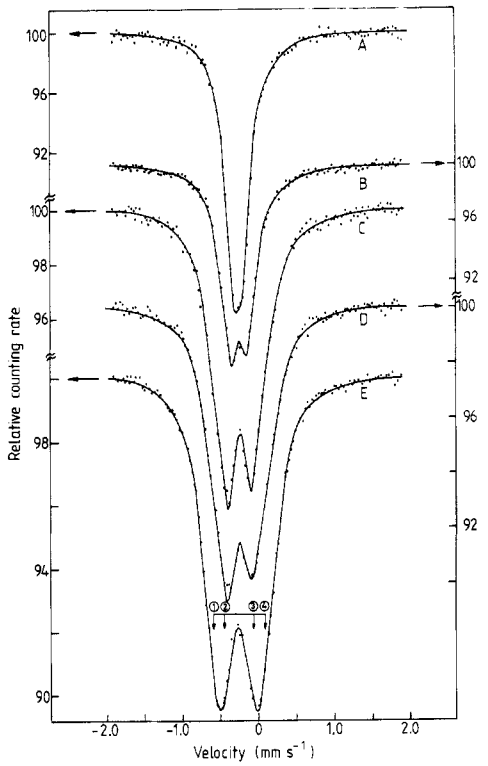

Figure 4. Room-temperature Mössbauer spectra of $Mg[Mg((CH_2)_6N_4)_2Fe(CN)_6]_2.nH_2O$ for different stages of hydration. The degree of hydration depends on the treatment temperature indicated in the figure. A: $T = 45$ °C; B: $T = 65$ °C; C: $T = 78$ °C; D: $T = 88$ °C; E: $T = 100$ °C.

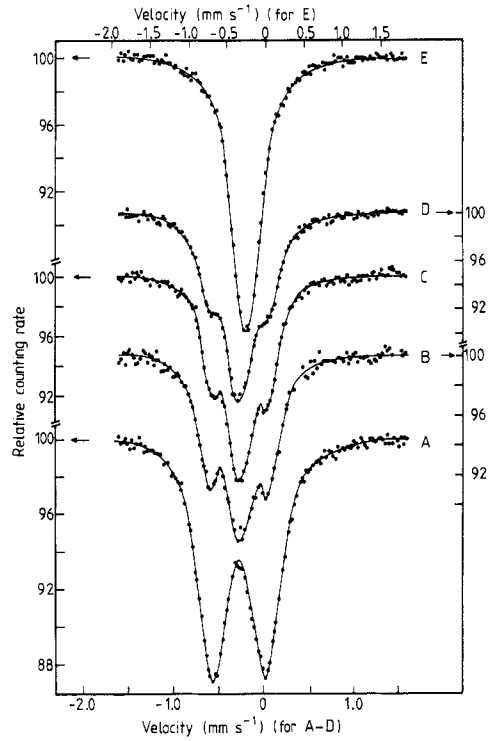

Figure 5. Mössbauer spectra exhibiting changes due to the gradual inclusion of water with time from the dehydrated stage (spectrum A) to different hydrated stages (spectra B–E). The samples for spectrum A, which had been heated at 100 °C (under vacuum), were kept under water for 3 d (spectrum B), 5 d (spectrum C), 8 d (spectrum D) and 15 d (spectrum E). (The velocity scales are the same for spectra A–D and different for spectrum E.)

this process for each treatment temperature a well defined specimen so far as the water content is concerned, is produced. The specimens at this stage do not contain water molecules which have bonding energies lower than a characteristic value determined by the treatment temperature. The situation is different in the case of rehydration. Here the completely dehydrated specimen is immersed in water at room temperature, enabling water molecules to enter the specimen at different rates depending on the different locations that they occupy. As the rehydration process proceeds, inhomogeneities may be created as a result of occupation of the various sites by the water molecules at different speeds. This non-equilibrium state of the sample will ultimately reach an equilibrium state after a long time (greater than 15 d) when all the sites are occupied and the sample becomes completely hydrated. This phenomenon can equivalently be described by the propagation of the hydration front from the surface of the specimen to the whole of the layered structure. From the detailed description given above, it is clear that the very distinction between the dehydration and the rehydration

processes prevents one from preparing identical specimens in the above two processes. This explains the dissimilarity of the spectra for the intermediate stages in figures 4 and 5.

The most striking spectral features of the specimen in the intermediate stages between complete hydration and dehydration are the asymmetries in the spectra and the changes in shape with dehydration. This peculiarity needs an explanation.

3.3. Method of analysis

Consideration of the structure reveals a non-equivalence of the local environment of iron atoms, at least in respect of their neighbouring guest species in the van der Waals gap. These guest species have a strong influence on the Fe site. There are two iron sites with equal proportions such that two discrete doublets are required to describe the asymmetric spectra of the sample. One type of ferricyanide group has all water molecules on both sides in the van der Waals gap (figure 1, line 2) while the other type (figure 1, line 1) has a Mg^{2+} ion and water molecules on both sides.

All the spectra are fitted with a least-squares spectral curve-fitting routine (Meerwall 1975) assuming Lorentzian lineshapes with free parameter first and then with different constraints. The data points are fitted from an initial guess of the position, linewidth and height of each resonance line.

For the spectrum of the completely hydrated sample (at room temperature), fitting with a single line offers large value for the goodness-of-fit parameter χ^2 and the minimum value of χ^2 is always obtained by fitting with two strongly overlapping Lorentzian lines and any attempt to fit this spectrum with more lines by using either free parameters or alternative constraints on the line positions and the linewidths, or on the intensity ratios failed. Not only does the fitting of the spectrum for the completely hydrated sample considering four lines give a high value of χ^2, but also the linewidths for all the lines decrease less than the natural width of iron metal observed in our instrument. The fitting with a single line gives χ^2 (per degree of freedom) equal to 1.91 while fitting with two lines gives $\chi^2 = 0.86$. So the computer analysis of the unresolved spectrum of the completely hydrated sample is consistent with two lines of equal intensity. It was found that, for the quadrupole-split spectrum of the dehydrated sample, the best fitting is always obtained with four Lorentzian lines. For the dehydrated sample the best χ^2 value considering two lines is 1.36 whereas this value becomes 0.68 when four lines are considered. So we can explain the four lines as the two doublets corresponding to the two iron sites. This is in agreement with the structural data which suggest that there will be a superposition of two doublets corresponding to two different iron sites. The intensities of the two inner lines are identical whereas the intensities of the outer pair are nearly equal and slightly smaller than the inner pair. The positions of these lines are shown in only one spectrum in figure 4 by a bar diagram. Moreover, the spectra presented in figure 5 for the rehydration studies consist of two small and narrow lines on the two sides of a broad and intense line which may be looked upon as a superposition of two lines not yet resolved. These features indicate the presence of four lines in the spectra for all samples except that for the completely hydrated sample. Now the four lines in figure 4 may be considered as the superposition of two nested symmetrical quadrupole-split doublets with almost equal isomer shifts, i.e. the inner lines (2 and 3) form one doublet and the outer lines (1 and 4) with slightly smaller but equal intensities form another doublet. With this assumption the areas under the two types of doublet become different. This will, on the other hand, lead us to assume either a difference in the

number of iron ions in the two sites with equal Lamb–Mössbauer factor f or a difference in the value of Lamb–Mössbauer factor f of the two iron sites which are equal in number. Since the structural information contradicts the first assumption, we are left with the second assumption. Now the Lamb–Mössbauer factor f may be expressed as

$$f = f_M f_K$$

where f_M is the Lamb–Mössbauer factor connected with the vibration of the molecule and f_K that connected with the vibration within the molecule (Vertes *et al* 1979). In the case of our complex compound the coordinate bonding of the central metal atom to the ligands is stronger than the van der Waals forces between the complex molecules. Therefore the intramolecular bonding is substantially stronger, i.e. $f_K > f_M$. Now the basic $[Fe(CN)_6]^{3-}$ complex anion in the two sites should have almost identical f_K. To our knowledge, the f-factor can have different values in different sites only if the Mössbauer nuclei in these sites have different coordinations around them (Grushko *et al* 1971). The changes in the environment around $[Fe(CN)_6]^{3-}$ in the two sites produced by the guest molecules cannot alter the values of f_M in the two sites sufficiently to explain the fact that the intensity of one doublet is about 70% of that of the other. Moreover, for layer structures the intensity asymmetry of the quadrupole-split doublet is almost a universal characteristic feature. There are many examples where such asymmetry appears in the case of layered (intercalated) compounds, e.g. caesium–graphite intercalation compound (Campbell *et al* 1977), Fe_xNbS_2 (Sundararajan *et al* 1983), $FePS_3$ (Chandra and Ericsson 1979, Bjarman *et al* 1983), Fe_xTaS_2 (Eibschutz *et al* 1975) and $Li_xV_{1-y}Fe_yS_2$ (Eibschutz *et al* 1980). So we can discard the assignment wherein the four lines are grouped together into two symmetrical doublets now, if we take one small line and a large line (i.e. lines 1 and 3, or lines 2 and 4) as a doublet, the areas under the doublet are always equal. This assignment shows an intensity asymmetry of the two peaks in each doublet. The intensity asymmetry of any resultant spectrum in the intermediate stage may be attributed to the superposition of the two presumably asymmetric doublets which have slightly different isomer shifts.

3.4. Asymmetry of doublets

The asymmetry in the intensity of a quadrupole-split Mössbauer spectrum of powdered samples may arise from the relaxation effect of paramagnetic ions (Blume 1965, Blume and Tjon 1968, Thrane 1971, Caplan and Carroll 1976), saturation or absorber thickness effect (Shenoy and Friedt 1973, 1974), preferred crystal orientation or texture effect (Gonser and Pfannes 1974) and the Goldanskii–Karyagin Effect (GKE) (Goldanskii and Makarov 1968). It is highly improbable that the relaxation phenomenon has any effect on the intensity ratio of the lines observed at room temperature. The spectrum of completely hydrated samples, recorded at a low temperature, showed no marked change from that at room temperature. This fact rules out the possibility of a relaxation effect. The GKE and the absorber thickness effect may contribute to the intensity asymmetry in a similar manner. Again, since the layered cyanide crystallises from solution in the form of a yellow precipitate, it may be suspected that a residual crystal orientation effect arising from crystallisation and recrystallisation might influence the shape of the spectrum. So to ascertain the cause of asymmetry we studied the samples in different ways. We studied two samples with different thicknesses of which sample 1 has thickness of 4.9 mg cm^{-2} and sample 2 contains 9.77 mg cm^{-2} of Fe. The intensity asymmetry due to the texture effect is generally temperature independent in nature and may be removed by carefully

grinding the sample (Herber and Chandra 1970). The sample was also mixed with fine glass powder and was ground to achieve random orientation of crystallites. Henceforth we shall mark the sample mixed with pyrex glass in the ratio 1:1 by weight as sample 3 and the sample prepared by mixing with Pyrex glass in the ratio 1:2 by weight as the sample 4. Table 1 summarises the ^{57}Fe Mössbauer data of sample 1. Since the isomer shift and quadrupole splitting values do not differ much for the four samples studied, we are presenting here the data of one sample only. Let us represent the asymmetry of the doublet by $R = A_+/A_-$, where A_+ and A_- are the areas of the split lines onto the positive and negative side, respectively, with respect to the centroid of the spectrum. In the range of thicknesses studied, the results of samples 1 and 2 show a little difference in the value of R, which may be attributed to the effect of thickness on the width of the line. The intensity ratio R is essentially the same both for an absorber made from the pure specimen and for an absorber prepared by mixing the pure sample with Pyrex glass powder. From the data on samples 3 and 4 it is seen that R is invariant with respect to the ferricyanide: Pyrex ratio, indicating that the crystal orientation effects are negligible in these samples.

In the case of axial symmetry if the z axis coincides with the crystal axis of symmetry $\langle x^2\rangle = \langle y^2\rangle = \langle x_\perp^2\rangle$ and $\langle z^2\rangle = \langle x_\parallel^2\rangle$, the Mössbauer recoilless fraction takes the form (Goldanskii and Makarov 1968)

$$f(\theta) = \exp[-k^2(\langle x_\parallel^2\rangle - \langle x_\perp^2\rangle)\cos^2\theta - k^2\langle x_\perp^2\rangle] = \exp(-k^2\langle x_\perp^2\rangle)\exp(-\varepsilon\cos^2\theta)$$

where $\varepsilon(= k^2(\langle x_\parallel^2\rangle - \langle x_\perp^2\rangle))$ is the lattice anisotropy parameter and k represents the magnitude of the wavevector. In the case of axial symmetry of the electric field gradient (EFG) and the Debye–Waller factor, the intensity asymmetry parameter may be written as

$$A = M_\pi/M_\sigma = \int_0^\pi [\exp(-\varepsilon\cos^2\theta)](1+\cos^2\theta)\sin\theta\,\mathrm{d}\theta \Big/ \int_0^\pi [\exp(-\varepsilon\cos^2\theta)] \times (5/3 - \cos^2\theta)\sin\theta\,\mathrm{d}\theta \neq 1$$

where M_π and M_σ are the intensities corresponding to the transitions with $\Delta m = 1$ and $\Delta m = 0$, respectively. The identification of the π- and σ-transitions helps to relate the parameters R and A. In our case the assignments of these transitions is not possible since the sign of V_{zz} is not known. In the case of GKE a strong temperature dependence of R is usually observed but in our case the temperature dependence is not so prominent. The Mössbauer measurements were also carried out at different temperatures from room temperature to 104 K with the sample prepared by heating at 88 °C (partially dehydrated). The spectra (figure 6) in this study show a small temperature dependence of the two peaks. In the case of GKE, usually the intensities of the two peaks of the quadrupole-split doublet move towards equalisation as the temperature is lowered. Hence from the above experimental observations it is reasonable to attribute the observed temperature-dependent asymmetry of intensity to the GKE which is the property of many highly anisotropic layered materials. The asymmetry of the intensity in the present case for two different sites seems to be opposite in nature (in one case, $R > 1$ whereas, in the other, $R < 1$). It may happen that the intensity of the resonance lines of each doublet changes but their superposition does show a change towards symmetry (figure 6).

Figure 7 demonstrates the anisotropy of the two doublets for the specimens treated at various temperatures, corresponding to different stages of dehydration. Maximum anisotropy is exhibited at 45 °C corresponding to the stage of hydration with 17 water

Table 1. ^{57}Fe Mössbauer parameters of $Mg[Mg((CH_2)_6N_4)_2Fe(CN)_6]_2 . nH_2O$ (sample 1; thickness, 4.9 mg cm^{-2} of Fe) at various treatment temperatures. The isomer shift is relative to metallic iron. The errors in the isomer shift and quadrupole splitting are ±0.01 mm s^{-1}.

Treatment temperature (°C)	Isomer shift (mm s^{-1})		Quadrupole splitting (mm s^{-1})		Number of peaks	Width (mm s^{-1})	Area under the curve (%)	Area ratio R	
	Doublet 1 (peaks 1 and 3)	Doublet 2 (peaks 2 and 4)	Doublet 1	Doublet 2				Doublet 1 (A_3/A_1)	Doublet 2 (A_4/A_2)
Room	−0.28	−0.26	—	—	1	0.24	48.83	—	—
					2	0.26	51.17		
45	−0.28	−0.26	0.16	0.16	1	0.28	20.49	1.425	0.709
					2	0.29	29.43		
					3	0.28	29.20		
					4	0.26	20.88		
65	−0.29	−0.20	0.30	0.35	1	0.37	21.30	1.353	0.749
					2	0.27	28.53		
					3	0.28	28.81		
					4	0.38	21.36		
78	−0.32	−0.17	0.39	0.46	1	0.40	22.17	1.285	0.757
					2	0.27	28.08		
					3	0.29	28.49		
					4	0.39	21.26		
88	−0.34	−0.17	0.46	0.47	1	0.42	23.80	1.102	0.896
					2	0.33	26.36		
					3	0.32	26.22		
					4	0.43	23.62		
100	−0.33	−0.17	0.52	0.54	1	0.42	24.22	1.061	0.971
					2	0.35	25.41		
					3	0.36	25.70		
					4	0.43	24.67		

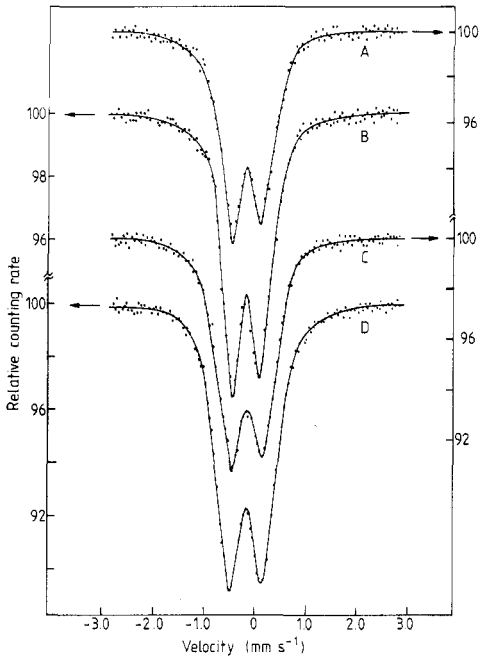

Figure 6. The temperature dependence of the Mössbauer pattern of the sample heated at 88 °C; spectrum A, 185 K; spectrum B, 168 K; spectrum C, 140 K; spectrum D, 104 K.

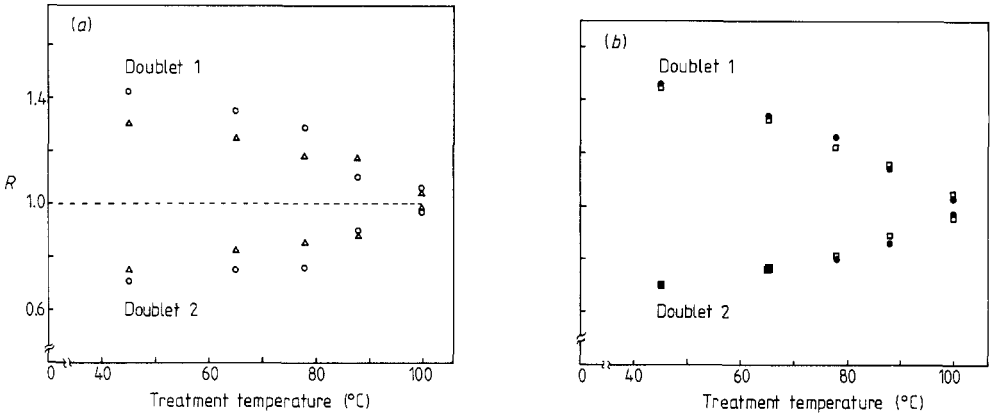

Figure 7. Area ratio $R(= I_+/I_-)$ versus treatment temperatures for samples with different thicknesses (*a*) (samples 1 (○) and 2 (△)). The asymmetry of the quadrupole lines (area ratio R) versus treatment temperatures for the compounds mixed with the Pyrex powder in two different ratios (*b*) (samples 3 (□) and 4 (●)).

molecules. This anisotropy goes on decreasing with further loss of water and almost vanishes when the treatment temperature is 100 °C (under vacuum) corresponding to a cubic structure of the lattice. The disappearance of anisotropy is quite understandable in the dehydrated cubic phase where the bonding along the *c* axis becomes strengthened because of the contraction of the *c* axis and consequently a drastic reduction in the lattice vibrational anisotropy occurs. The anisotropy of the two doublets is, however, opposite

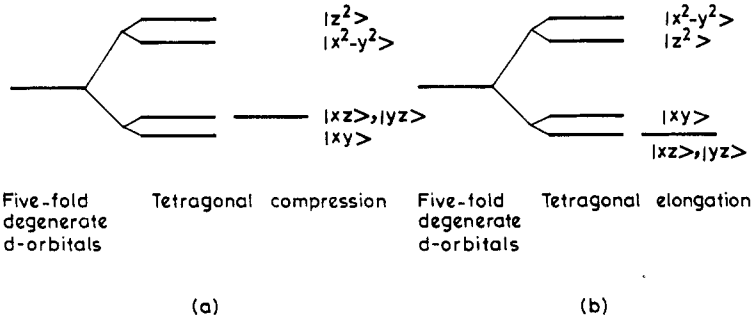

Figure 8. Electronic configurations for iron in cubic ligand fields with tetragonal distortion.

in nature. This feature needs an explanation. The opposite nature of anisotropy of the doublets arising from iron at the two sites (at line 1 and line 2) in figure 1 may be attributed either to the opposite sign of EFG or to the sign of $\varepsilon(= k^2(\langle x_\parallel^2\rangle - \langle x_\perp^2\rangle))$ at the two sites. Since strong molecular forces operate along the *a–b* plane for both the sites of iron ions, the anisotropy of the lattice vibration for both the sites represented by ε is supposed to have the same sign. Accordingly, the EFGs at the two sites would have to be of opposite signs.

3.5. *Origin of EFG*

The quadrupole splitting ΔE_Q is given by

$$\Delta E_Q = \tfrac{1}{2}e^2qQ(1 + \eta^2/3)^{1/2}$$

where Q is the quadrupole moment and η is the asymmetry parameter ($\eta = 0$, in axial case). The total EFG may be considered to originate partly from the non-cubic electronic distribution in partially filled valence orbitals of iron atoms and partly from the anisotropic arrangement of the charges on the surrounding ions in the lattice. Therefore the total effective EFG may be written as (Ingalls 1964)

$$q = (1 - R)q_{\text{val}} + (1 - \gamma_\infty)q_{\text{lat}}$$

where R and γ_∞ are Sternheimer shielding and antishielding factors. In an octahedral field, the fivefold degenerate d orbitals are split into a doubly degenerate e_g ($d_{x^2-y^2}$, d_{z^2}) and a triply degenerate t_{2g} (d_{xy}, d_{yz}, d_{zx}) level. For low-spin Fe(III) in a cubic field of octahedral symmetry the separation between e_g and t_{2g} levels is so large that all the valence electrons will be populated in the threefold t_{2g} levels and this symmetrical distribution of the electrons in the t_{2g} levels will contribute nothing to q_{val}. Since a large number of water molecules, executing vibrational and librational motion, surround the $Fe(CN)_6$ group, the Fe ion is effectively screened by these molecules whereby the EFG produced by the lattice charges does not impart any effect on the Fe nuclei. The Mössbauer spectrum for low-spin Fe(III) in such a symmetric environment will show a single line. The splitting of the t_{2g} levels due to tetragonal elongation and contraction is shown in figure 8. It should also be mentioned here that spin–orbit coupling plays an important role in determining the electronic ground state of the low-spin $3d^5$ electronic configuration. The spin–orbit interaction causes an admixture of excited states in the ground state and has a considerable effect on the quadrupole splitting at low

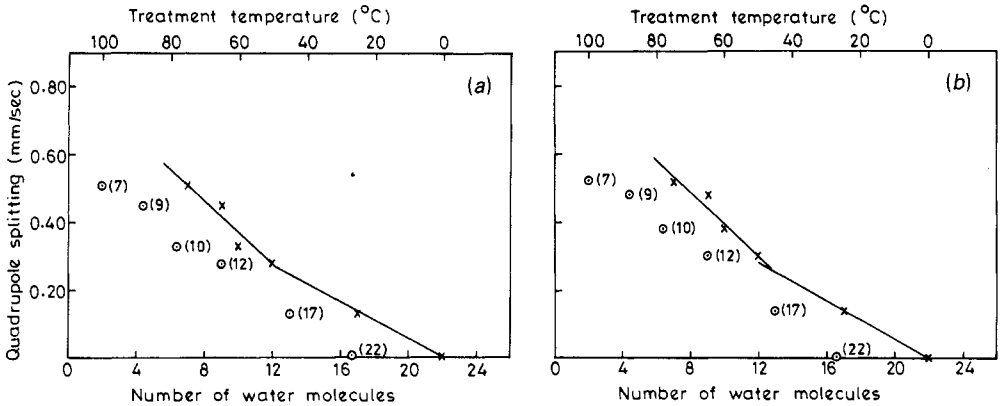

Figure 9. Variation in quadrupole splitting for sample 4 as a function of the number of water molecules (×) and treatment temperatures (⊙) in magnesium hexamethylene tetramine ferricyanide: (*a*) doublet 1; (*b*) doublet 2. The numbers in parentheses represent the number of water molecules present.

temperatures (Ingalls 1964). Since the paper is concerned with a qualitative, rather than a quantitative interpretation, the effect of the spin–orbit interaction has not been taken into account.

In the present case the origin of the EFG with different signs at two sites may be explained as follows: $Fe(CN)_6$ groups at line 1 are expected to be elongated because of the proximity of Mg^{2+} ions in the van der Waals gap, while the $Fe(CN)_6$ octahedra at line 2 of figure 1 will experience a contraction along the *c* axis. This will cause a difference in the relative positions of the t_{2g} levels as shown in figure 8. The valence contribution to EFG by five electrons (t_{2g}^5) for a Fe site on line 1 of figure 1 is $-\frac{4}{7}\langle r^{-3}\rangle$ because the contribution of the first three electrons in the three t_{2g} levels cancels out. Similarly the EFG at Fe located on line 2 is equal to $+\frac{2}{7}\langle r^{-3}\rangle$. Although this empirical calculation explains the opposite sign of the EFG, it stipulates a quantitative relation whereby the splitting of one doublet will be double that of the other. Our results, however, do not uphold this exact quantitative relationship because it is modified by the lattice part of the EFG. So, to summarise, when the specimen is completely hydrated, there are almost 24 water molecules present in the molecule. These water molecules create a symmetric environment about the $Fe(CN)_6$ group and make the iron site feel an almost cubic octahedral field. This gives rise to a single line in the Mössbauer spectrum for a basically trivalent iron ion in the low-spin configuration. With the progressive dehydration, tetragonal distortion (elongation or contraction) gradually appears, causing a partial lift in the degeneracy of the t_{2g} levels. The electronic distribution in these levels contributes to the valence part and a splitting in the Mössbauer spectrum develops and increases in magnitude with gradual dehydration.

3.6. Variation in quadrupolar splitting and isomer shifts

In figure 9, we have presented the variation in the quadrupole splitting of the two doublets as a function of the number of water molecules and treatment temperatures (in figure 9, we have presented only one representative curve because the curves are identical in nature for all the samples). Since the relation between the quadrupole

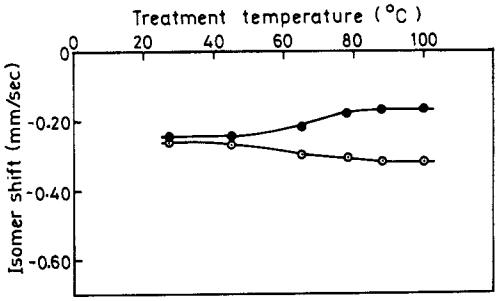

Figure 10. Isomer shift versus treatment temperatures for sample 3: ⊙, doublet 1; ●, doublet 2.

splitting and the hydration number is linear but follows two different straight lines for both the doublets, this leads us to believe the existence of different binding energies for different groups of water molecules as was found from the TGA (Weiss *et al* 1953). The quadrupole splitting is found to increase with decrease in the number of water molecules. The quadrupole splitting is found to increase in the case of sodium nitroprusside heated at higher temperatures, indicating an EFG difference at the Fe site of hydrated and dehydrated sodium nitroprusside (Boughton *et al* 1976, Long *et al* 1978). The s-electron density is also found to change by the removal of water molecules although they are not directly bonded to the iron nucleus. Similar behaviour was found in the case of $(C_6H_5)_2SnCl_2 . nH_2O$ molecule when $n \leqslant 6$ (Balabanov *et al* 1971). The quadrupole-splitting value of this sample increases markedly with decrease in the water content due to the strong distortion of the electric field and the increase in the EFG. With increase in the water content, the water molecules surround the $(C_6H_5)_2SnCl_2$ molecule more uniformly and reduce the EFG. In our case, 24 water molecules per formula unit play the above role more efficiently. These examples support the above model depicted to explain the experimental observations.

The isomer shift of iron for two inequivalent sites as obtained from least-squares fitting is shown in figure 10 as a function of treatment temperature. In all cases the isomer shift values for the two doublets differ by about 0.17 mm s^{-1} in the completely dehydrated case and then gradually converge on increase in the number of water molecules to a common value of -0.27 mm s^{-1}. In the completely hydrated specimen the lattice parameters are $a = 10.5$ Å and $c = 33.3$ Å. The interaction of water molecules extends the axis to a great extent. The effect of 24 water molecules exerts the dominant role, thereby screening out the effect of the Mg^{2+} ion on the iron atom in line 1 of figure 1 as well as the effect of hexamethyline tetramine (HMT) on the iron atom on line 2 of figure 1. As a result the isomer shift which is basically dependent on the charge density of s electrons at the iron atom becomes almost identical (a very small difference in the isomer shift for two distinguishable sites). As the water molecules are being progressively expelled from the lattice on heating, the effect of the Mg^{2+} ion and HMT is further enhanced by contraction of the lattice. On the assumption that the polarising effects of Mg^{2+} and HMT (outer-sphere coordination complex) on iron atoms in two sites are different both in sign and in magnitude, the asymmetric variation in isomer shift in the opposite direction as shown in figure 10 is qualitatively understood (Fluck 1968).

The line widths (full width at half-maximum) of lines 2 and 3 of figure 4 are equal and those of lines 1 and 4 of figure 4 are also identical. The latter pair are wider than the former pair because of the influence of GKE (Balabanov *et al* 1971). On increase in the

number of water molecules the widths of all the resonance lines decrease. The hydrated state gives rise to the most uniform local symmetry and the dehydration introduces strains in the lattice due to random environmental configurations which may be responsible for the fact that the spread in the value of the splitting varies from site to site. This will cause a broadening of the individual lines.

It is interesting to note a parallelism between resistivity and quadrupole splitting both as a function of temperature. The change in slope in figure 3 and figure 9 may be correlated. When water molecules are expelled from the specimen, the lattice contracts. At a particular stage of dehydration around 60 °C, the local symmetry of the Fe^{3+} ion is disturbed rather abruptly. Thus the point where the slopes of the resistivity curve and the quadrupole splitting versus temperature curve changes may be indicative of a minor structural phase transition. So all the interactions (mentioned above) operating together nicely explain the appearance and disappearance of splitting together with the behaviour of resistivity, quadrupole splitting and the anisotropy at various treatment temperatures.

4. Conclusion

From the experimental results the following conclusions can be drawn about the behaviour of the layered ferricyanide.

(i) Water molecules reside in this layered cyanide as guest molecules and are expelled on heating, not continuously but in steps. The process of intercalation of water is reversible.

(ii) Although the Mössbauer spectrum shows a single line in the hydrated form and a quadrupole-split doublet in the dehydrated form, iron exists in the trivalent state in both situations. The splitting collapses in the hydrated state owing to symmetric field about the iron ion, produced by the uniform surroundings created by a large number of water molecules.

(iii) The intensity asymmetry of the quadrupole-split doublets can be attributed to the GKE.

The present investigation of a layered cyanide provides an elegant system wherein one third of the Mg^{2+} ions which reside in the van der Waals gap may be replaced by NH_4^+, Li^+, Co^{2+}, Ni^{2+}, Cu^{2+}, etc, and the water molecules may be replaced by polar organic molecules such as aniline, acetone or alcohol, creating a new family of tailor-made substances where the expected anisotropic properties could be investigated by various techniques.

References

Balabanov N, Komissarova B A, Sorokin A A and Shpinel V S 1971 *Proc. Conf. on the Applications of the Mössbauer Effect (Tihany, 1969)* ed I Dezsi (Budapest: Akademiai Kiado) p 235

Bjarman S, Jernberg P and Wappling R 1983 *Hyperfine Interact.* **16** 625

Blume M 1965 *Phys. Lett.* **14** 96

Blume M and Tjon J A 1968 *Phys. Rev.* **165** 446

Boughton C A, Bradley G R, Matejczyk D E, Reed C R, McKinney B J and Lombardi J C 1976 *J. Inorg. Nucl. Chem.* **38** 427

Campbell L E, Montel G L and Perlow G J 1977 *Phys. Rev.* B **15** 3318

Caplan M and Carroll T X 1971 *Proc. Conf. on the Applications of the Mössbauer Effect (Tihany, 1969)* ed I Dezsi (Budapest: Akademiai Kiado) p 169

Chandra R and Ericsson T 1979 *Hyperfine Interact.* **7** 229
Das S, Bhattacharya M and Bhattacharya R L 1983 *Cryogenics* **23** 479
Das S, Ganguli S and Bhattacharya M 1985 *J. Phys. C: Solid State Phys.* **18** 3809
Eibschutz M, Murphy D W and DiSalvo F J 1980 *Physica* B–C **99** 145
Eibschutz M, DiSalvo F J, Hull G H and Mahajan S 1975 *Appl. Phys. Lett.* **27** 464
Fluck E 1968 *Chemical Applications of Mössbauer Spectroscopy* ed V I Goldanskii and R H Herber (New York: Academic) p 207
Goldanskii V I and Makarov E F 1968 *Chemical Applications of Mössbauer Spectroscopy* ed V I Goldanskii and R H Herber (New York: Academic) p 102
Gonser U and Pfannes H D 1974 *J. Physique Coll.* **35** C6 113
Grushko Y S, Lurie B G and Murin A N 1971 *Proc. Conf. on the Applications of the Mössbauer Effect (Tihany, 1969)* ed I Dezsi (Budapest: Akademiai Kiado) p 681
Herber R H and Chandra S 1970 *J. Chem. Phys.* **52** 6045
Ingalls R I 1964 *Phys. Rev.* **133** A787
Levy F (ed) 1979 *Intercalated Layered Materials* (Dordrecht: Reidel) p 99
Long J C, Thomas J L and Lombardi J C 1978 *J. Inorg. Nucl. Chem.* **40** 1627
Meerwall E V 1975 *Comput. Phys. Commun.* **9** 117
Schollhorn R 1980 *Physica* **99** 89
Shenoy G K and Friedt J M 1973 *Phys. Rev. Lett.* **31** 419
—— 1974 *Nucl. Instrum. Methods* **116** 573
Sundarajan M D, Narayansamy A, Nagarajan T, Sunandana C, Subba Rao G V, Niarchos D and Shenoy G K 1983 *J. Phys. Chem. Solids* **44** 773
Thrane N 1971 *Proc. Conf. on the Applications of the Mössbauer Effect (Tihany, 1969)* ed I Dezsi (Budapest: Akademiai Kiado) p 175
Vertes A, Korecz L and Burger K 1979 *Mössbauer Spectroscopy, Studies in Physical and Theoretical Chemistry* vol 5 (New York: Elsevier) p 21
Weiss V A, Weiss A and Hofmann U 1953 *Z. Anorg. (Allg.) Chemie* **273** 129
Whittingham M S 1978 *Prog. Solid State Chem.* **12** 41
Whittingham M S and Jacobson A (ed) 1982 *Intercalation Chemistry* (New York: Academic) p 573
Wilson J A, Disalvo F J and Mahajan S 1975 *Adv. Phys.* **24** 117
Wilson J A and Yoffe A D 1969 *Adv. Phys.* **18** 193